

A Modified Harmonics Reduction Technique for a Three-Phase Controlled Converter

Ali M. Eltamaly

Abstract—Three-phase controlled converters have many applications especially in adjustable speed drives and renewable energy. A three-phase controlled converter is a good option in these applications due to its low cost, simplicity, and maintainability with respect to other solutions like a full-bridge insulated gate bipolar transistor converter or a Vienna rectifier. Line current harmonics in this converter is very high; therefore, a harmonics reduction technique is needed to remedy the problem. In this paper, an improved injection current technique is introduced to reduce line current harmonics. The optimal amplitude and phase angle of the injection current for different loads and firing angles have been mathematically determined. Simulation for this technique has been performed by using the PSIM simulation program. An experimental prototype has been built to verify the mathematical and simulation results. The simulation and experimental results show a sensitive variation in the total harmonic distortion of the line current for the amplitude and angle of injection current variations. The simulation and experimental results prove the superiority of this technique in mitigating the requirements for harmonics standards.

Index Terms—Harmonics, third harmonic injection, three-phase controlled converter.

I. INTRODUCTION

IN MODERN power electronics converters, a three-phase controlled converter is commonly used especially as a rectifier in interfacing adjustable speed drives (ASD) [1]–[4] and renewable energy in electric utilities [5], [6]. The three-phase controlled converter has a simple construction and control, low cost, and low acoustic noise compared with other solutions like full-bridge insulated gate bipolar transistor line side inverters or Vienna rectifiers. The line current of a controlled converter and its fast Fourier transform (FFT) components are shown in Fig. 1. It is clear from this waveform that this converter generates high harmonics in the line currents which distort the voltage at the point of common coupling in the power system. A lot of efforts have been performed to reduce harmonic contents in the utility line currents of controlled converters [7]–[27]. Passive filters have been used in many researches with different configurations [7], [8], but this technique suffers from bulky, heavy filter elements and sometimes causes resonance problems. Active filters have been used in many researches and it seems to be an interesting option, but this technique suffers from complexity and high cost [9], [10]. Hybrid solutions

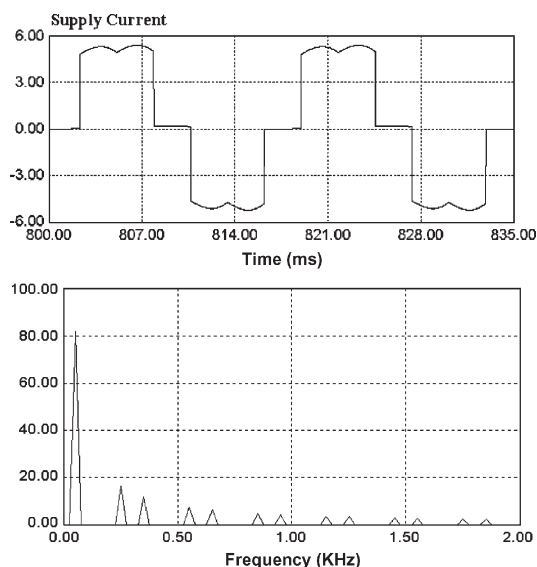


Fig. 1. Supply current and its FFT of controlled converter without any harmonic reduction means.

using active filters and passive filters are used in high-power applications to improve passive filter performance [11]. An increasing number of pulses [12]–[15] reduces the harmonic contents in a line current. However, this technique is heavy, has high cost, complex construction, needs to be large in size, and it is not readily available from the manufacturer [14]. Early work in third harmonic injection techniques have been used in [6], [8], [27]. Some other literatures use switches in the main path of power flow which increase the switching losses and reduce the system reliability [5]. Injection of third harmonic current to line currents can be achieved by using LC branches tuned around the third harmonic frequency [27]. However, this scheme suffers from bulky construction, resonant problems, and the current in the injection branch is very sensitive to the deviation of the L and C values. Most three-phase line current harmonics reduction techniques are summarized in [28], [29]. Injection of the third harmonic to a line current using a zigzag transformer has been shown in many researches [5], [17]–[27]. These researches and the ideas shown in this research show the superiority of this technique in reducing the harmonic contents of line currents and increasing the power factor of the controlled or uncontrolled converters.

II. PROPOSED APPROACH

Fig. 2 shows the topology of the proposed approach to reduce harmonics generated by a line commutated SCR inverter used

Manuscript received November 23, 2006; revised September 10, 2007.

The author is with the Department of Electrical Engineering, College of Engineering, King Saud University, Riyadh 11421, Saudi Arabia (e-mail: eltamaly@ksu.edu.sa).

Color versions of one or more of the figures in this paper are available online at <http://ieeexplore.ieee.org>.

Digital Object Identifier 10.1109/TIE.2007.908542

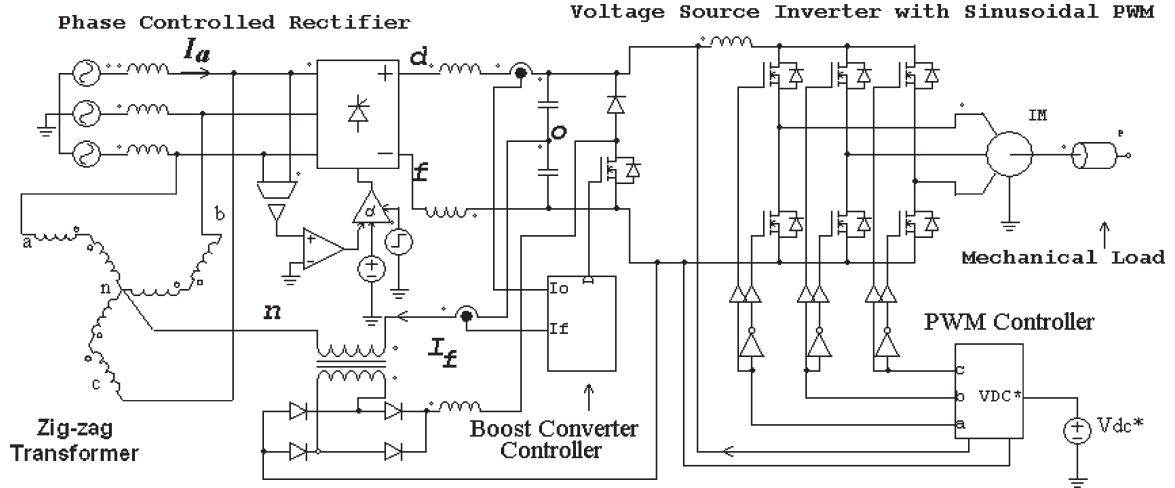


Fig. 2. Proposed approach.

in ASD. This approach contains a zigzag transformer that gives high impedance for the fundamental frequency component and very low impedance for the injection current. A single-phase transformer is connected between the dc-link mid-point “o” and the zigzag transformer neutral “n.” The secondary of single-phase transformer is connected to a rectifier boost converter stage feeding the dc link. The injected current I_f can be regulated by operating a single switch. The duty ratio of the boost converter can be varied to control the injection current depending on the dc link voltage.

The main goal of this paper is to obtain the optimal rms value and phase angle of the injection current to get the minimum total harmonic distortion (THD) of the supply current. Previous results indicate that the best rms value of the third harmonic current is equal to the average value of the dc link current [13], [14]. However, it is not the only condition required. The angle of injection current also plays a very important role in the THD of the line current. Therefore, it is important to determine the relation between the angle of injection current ψ and the firing angle α .

For firing angle $\alpha = 20^\circ$ (as an example), Fig. 3(a) shows the utility line current with respect to the voltage of phase “a”. Fig. 3(b) shows the third harmonic injection current with respect to phase a voltage. It is clear from this waveform that the injection current leads the phase a voltage by 120° , which agrees with the analysis and waveforms in the upcoming sections. Fig. 3(c) shows the line current with the third harmonic current along with the phase voltage a. This figure reveals that the angle between I_f and I_a must be 180° with respect to the third harmonic frequency. Fig. 3(d) shows the voltage between point “d” and “n” V_{dn} , the voltage between point “f” and “n” V_{fn} and the voltage between “o” and “n” V_{on} along with phase “a” voltage. The third harmonic components of the voltages V_{dn} , V_{fn} and V_{on} have been used to inject the third harmonic back to the utility line current to reduce the harmonic content. Therefore, a careful analysis of these voltages is required to get the optimum value of injection current and its angle ψ . It is convenient to employ the Fourier series in the analysis of

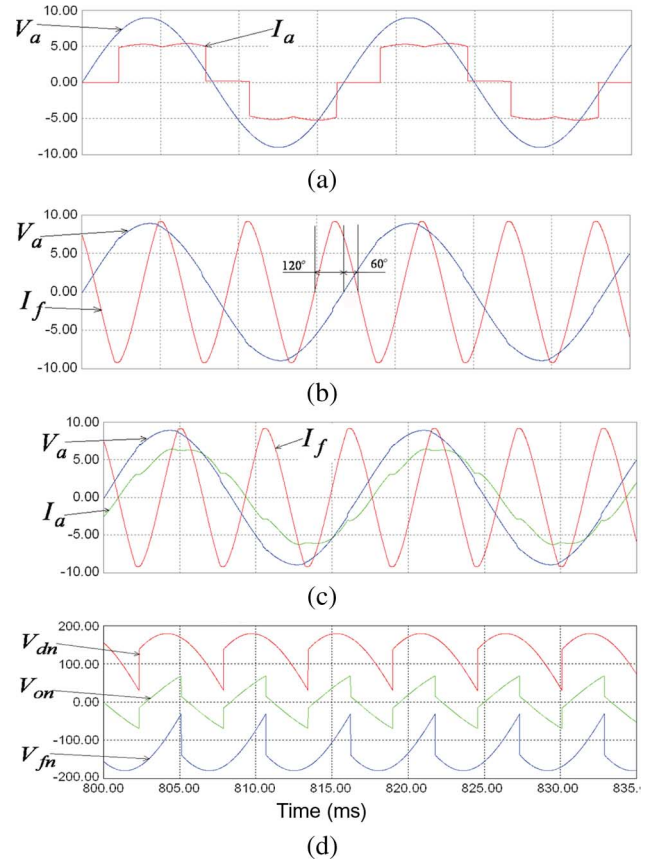


Fig. 3. Various voltages and currents of the proposed approach at $\alpha = 20^\circ$. (a) Voltage and current of phase a. (b) Voltage of phase a and reinjection current. (c) Voltage, current of phase a and reinjection current. (d) The voltages V_{dn} , V_{on} , and V_{fn} .

the distorted waveforms. In general, a nonsinusoidal waveform $f(\omega t)$ can be expressed as follows:

$$f(\omega t) = a_0 + \sum_{n=1}^{\infty} (a_n \cos(n\omega t) + b_n \sin(n\omega t))$$

where a_0 , a_n , and b_n are Fourier coefficients.

By applying Fourier equations to the waveforms of V_{dn} , the third harmonic component is obtained as follows:

$$a_3 = \frac{3}{\pi} \int_{\frac{\pi}{6} + \alpha}^{\frac{5\pi}{6} + \alpha} V_m \sin \omega t * \cos 3\omega t d\omega t$$

$$= \frac{3\sqrt{3} V_m}{8\pi} [2 \sin(2\alpha) - \sin(4\alpha)] \quad (1)$$

$$b_3 = \frac{3}{\pi} \int_{\frac{\pi}{6} + \alpha}^{\frac{5\pi}{6} + \alpha} V_m \sin \omega t * \sin 3\omega t d\omega t$$

$$= \frac{3\sqrt{3} V_m}{8\pi} [\cos(4\alpha) - 2 \cos(2\alpha)]. \quad (2)$$

From (1) and (2), V_{dn3} and its angle can be obtained as in (3) and (4)

$$V_{dn3} = \frac{1}{\sqrt{2}} * \sqrt{a_3^2 + b_3^2} = \frac{3V_{LL}}{8\pi} \sqrt{1 + 8 \sin^2 \alpha} \quad (3)$$

where

- V_m peak value of phase voltage;
- V_{LL} rms value of line to line supply voltage;
- V_{dn3} rms value of third harmonic of the voltage between points d and n .

And angle of V_{dn3} is

$$\tan^{-1} \left(\frac{a_3}{b_3} \right) = \tan^{-1} \left(\frac{2 \sin(2\alpha) - \sin(4\alpha)}{\cos(4\alpha) - 2 \cos(2\alpha)} \right). \quad (4)$$

In the same way, V_{fn3} can be obtained as follows:

$$a_3 = \frac{3}{\pi} \int_{\frac{7\pi}{6} + \alpha}^{\frac{11\pi}{6} + \alpha} V_m \sin \omega t * \cos 3\omega t d\omega t$$

$$= \frac{3\sqrt{3} V_m}{8\pi} [2 \sin(2\alpha) - \sin(4\alpha)] \quad (5)$$

$$b_3 = \frac{3}{\pi} \int_{\frac{7\pi}{6} + \alpha}^{\frac{11\pi}{6} + \alpha} V_m \sin \omega t * \sin 3\omega t d\omega t$$

$$= \frac{3\sqrt{3} V_m}{8\pi} [\cos(4\alpha) - 2 \cos(2\alpha)]. \quad (6)$$

From (5) and (6), V_{fn3} and its angle are obtained as in (7) and (8)

$$V_{fn3} = \frac{1}{\sqrt{2}} * \sqrt{a_3^2 + b_3^2} = \frac{3V_{LL}}{8\pi} \sqrt{1 + 8 \sin^2 \alpha}. \quad (7)$$

V_{fn3} is the rms value of the third harmonic of the voltage between points f and n and the angle of V_{fn3} is

$$\tan^{-1} \left(\frac{a_3}{b_3} \right) = \tan^{-1} \left(\frac{2 \sin(2\alpha) - \sin(4\alpha)}{\cos(4\alpha) - 2 \cos(2\alpha)} \right) \quad (8)$$

$$V_{on3} = \frac{V_{dn3} + V_{fn3}}{2}. \quad (9)$$

Then,

$$V_{on3} = \frac{3V_{LL}}{8\pi} \sqrt{1 + 8 \sin^2 \alpha} \quad (10)$$

and angle of V_{on3} , is

$$\theta = \tan^{-1} \left(\frac{a_3}{b_3} \right) = \tan^{-1} \left(\frac{2 \sin(2\alpha) - \sin(4\alpha)}{\cos(4\alpha) - 2 \cos(2\alpha)} \right) \quad (11)$$

$$I_f = \frac{V_{on3} \angle \theta}{Z \angle \psi} = \frac{V_{on3}}{Z} \angle (\theta - \psi) \quad (12)$$

where, V_{on3} is the rms value of the third harmonic of the voltage between points o and n , and, θ is the angle of V_{on3} , and, ψ is the angle between V_{on3} and I_f .

As shown in Fig. 3, the voltage V_a is taken as a reference value, so the phase angle of the fundamental and third harmonic components of phase a current are $-\alpha$ and -3α , respectively. As explained in [25] and as is clear from Fig. 3, the optimum phase difference between phase a current and injection current is 180° , then

$$(\theta - \psi_{opt}) - (-3\alpha) = 180 \Rightarrow \psi_{opt} = \theta + 3\alpha - 180. \quad (13)$$

From (13) and Fig. 3, the phase difference between each vector for various firing angles $\alpha = 20^\circ$ and 40° (as an example) is shown in Fig. 5. From (10) the relation between V_{on3} and the firing angle α is shown in Fig. 4. In the same way, from (13) the relation between the angle of V_{on3} and the angle between I_f , and ψ along with the firing angle α is shown in Fig. 5.

III. DESIGN EXAMPLE

Experimental and simulation verification for this technique has been carried out. The prototype model is used in the simulation and in the experiment. A dc link is connected with a three-phase pulsewidth modulation (PWM) inverter and 1-kW squirrel cage induction motor. For the controlled rectifier, the values of V_{on3} vary between $V_{on3}(\alpha = 0) = 0.1194$ p.u. to $V_{on3}(\alpha = 90^\circ) = 0.358$ p.u. At full load, the dc current $I_o = 0.6224$ p.u. The base voltage and current are 220 V and 3.3 A, respectively.

The simulation results in the next section reveals that the minimum THD occurs almost at $I_f/I_o = 1.25$, so at full load; $I_f = 0.8$ p.u. The rated third harmonic current passing through the zigzag transformer is $I_f/3 = 0.2667$ p.u. The value of I_f is controlled depending on the value of the dc link current for minimum THD. The third harmonic injection current can be controlled by controlling the duty ratio of the boost converter. A current sensor is used to measure the actual dc link current and the third harmonic injection current. The error signal between these two currents is used to control the duty ratio of the boost converter. 10 kHz switching frequency of the boost converter is used in simulation and in the practical prototype. The schematic of the controlled circuit of the boost converter is shown in Fig. 6.

Design of Single-Phase Transformer

The rated primary voltage of a single-phase transformer in the third harmonic injection pass is $V_{on3}(\alpha = 90) = 0.358$ p.u.

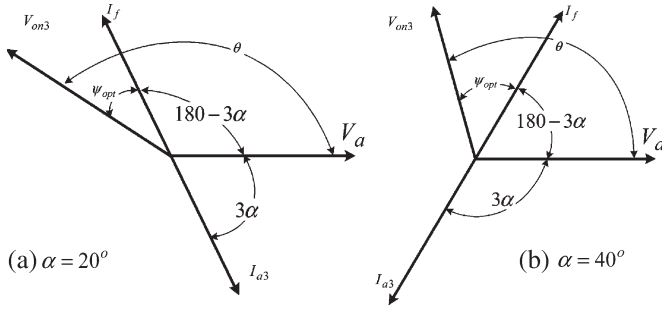


Fig. 4. Phase difference between each component for (a) $\alpha = 20^\circ$ and (b) $\alpha = 40^\circ$.

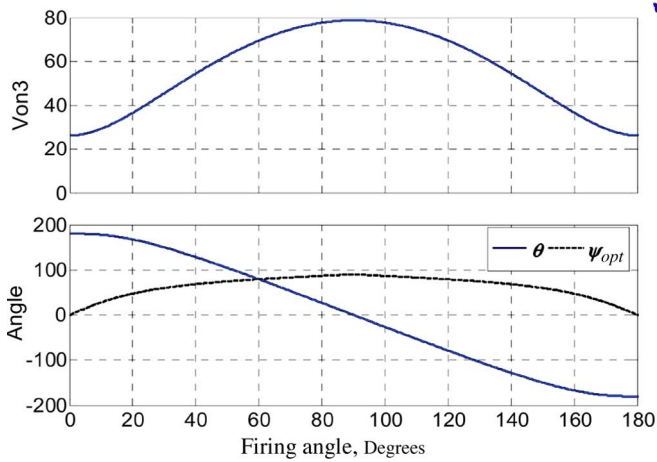


Fig. 5. Variation of V_{on3} , θ , ψ_{opt} with α at $V_{LL} = 220$ V.

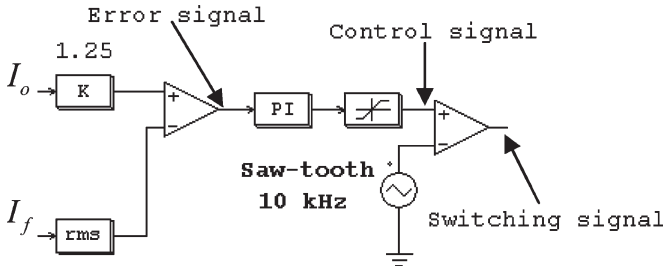


Fig. 6. Schematic of the control circuit of the boost converter.

Also, the rated primary current of this transformer is $I_f = 0.8$ p.u. Therefore, the rated kilovoltampere of this transformer is $0.8 * 0.358 = 0.286$ p.u.

The turns ratio of the step-up single-phase must handle the minimum value as well as the maximum value of V_{on3} . The minimum value of V_{on3} is at $\alpha = 0$, which is $V_{on3}(\alpha = 0) = 0.1194$ p.u. Then, the corresponding value of V'_{on3} is

$$V'_{on3}(\alpha = 0) = 0.1194/n \text{ p.u.} \quad (14)$$

The output dc voltage of the single-phase diode rectifier, V_{bi} is

$$V_{bi} = 2 * \sqrt{2} * V'_{on3}/\pi. \quad (15)$$

The minimum value of V_{on3} corresponds to the maximum value of the duty ratio of the boost converter. Assume the

maximum allowable value of the duty ratio is 0.8. Then, the output voltage of the boost converter, V_{bo} is

$$V_{bo} = V_{bi}/(1 - D). \quad (16)$$

Substitute the value of V_{bi} from (15) into (16) and $D = 0.8$, the following equation can be obtained

$$\begin{aligned} V_{bo}(D = 0.8) &= (2 * \sqrt{2} * V'_{on3}/\pi) / (1 - 0.8) \\ &= (10 * \sqrt{2} * V'_{on3}) / \pi. \end{aligned} \quad (17)$$

The output voltage from the boost converter must equal the dc link voltage. The dc link voltage is kept constant at 1.25 p.u. by controlling the firing angle of the controlled converter and the modulation index of the PWM inverter. Thus, by equating (17) with 2.2 p.u., the following equation can be obtained:

$$10 * \sqrt{2} * V'_{on3}/\pi = 2.2 \text{ p.u.}$$

Then

$$V'_{on3}(\alpha = 0) = 2.2 * \pi / (10\sqrt{2}) \text{ p.u.} \quad (18)$$

By equating the values of V'_{on3} in (14) and (18), the following equation can be obtained:

$$0.1194/n = 2.2 * \pi / (10\sqrt{2}).$$

Then, the turns ratio of the single-phase transformer is

$$n = 10\sqrt{2} * 0.1194 / (2.2 * \pi) = 0.24. \quad (19)$$

IV. SIMULATION AND EXPERIMENTAL RESULTS

The simulation of the proposed technique has been performed using the PSIM computer program [30]. The same values of the components used in the simulation program have been used in the experimental prototype to compare these results.

Fig. 7 shows the simulation and experimental results of the relation between THD and the value of I_f/I_o for different values of firing angle α . This figure reveals that the optimal value of I_f/I_o is about 1.25 for the best THD. Also, it is clear that the best THD is linearly proportional to the firing angle α . This figure shows the importance of the third harmonic injection technique especially for high values of firing angle α .

Fig. 8 shows the simulation and experimental results of the relation between THD and the angle of I_f with respect to V_{on} , ψ at $I_f/I_o = 1.25$ for different values of firing angle α . It is clear that the best THD occurs around ψ_{opt} , which is obtained from (13). The value of ψ_{opt} increases as the firing angle α increases. There is an interesting contrast between the results shown in Figs. 5 and 8 in the optimum value of the injection current for different values of α .

The simulation and experimental waveforms are shown for $\alpha = 20^\circ$ and 40° as an example.

A. Simulation and Experimental Results at $\alpha = 20^\circ$

Fig. 9 shows the waveforms of voltage V_{df} and V_{ab} . Fig. 10 shows the supply current waveform and its FFT components

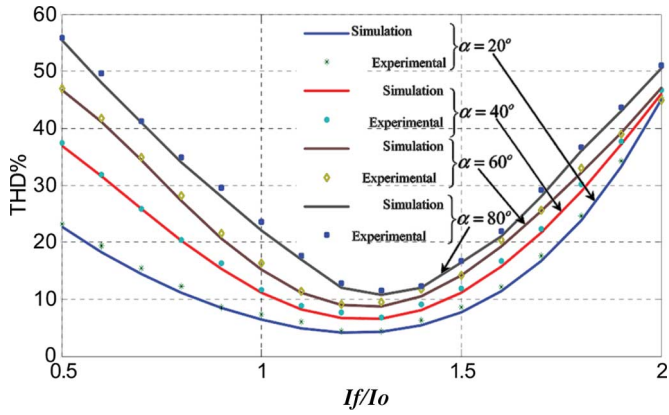


Fig. 7. Relation between THD and the value of I_f/I_o for different values of firing angle, α .

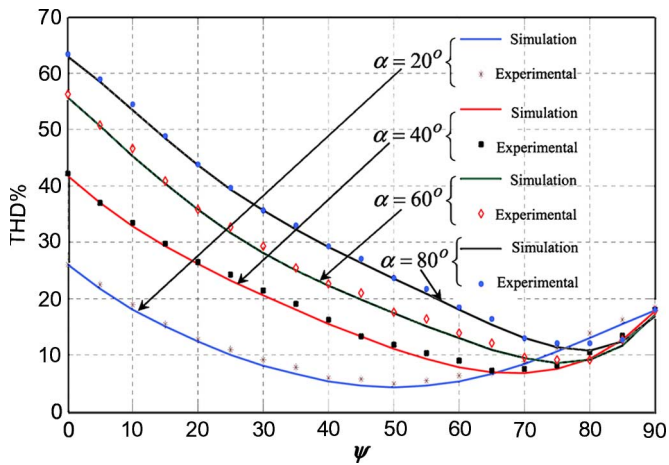


Fig. 8. Simulation and experimental results of the relation between THD and the angle of I_f with respect to V_{on} at $I_f/I_o = 1.25$ for different values of firing angle, α .

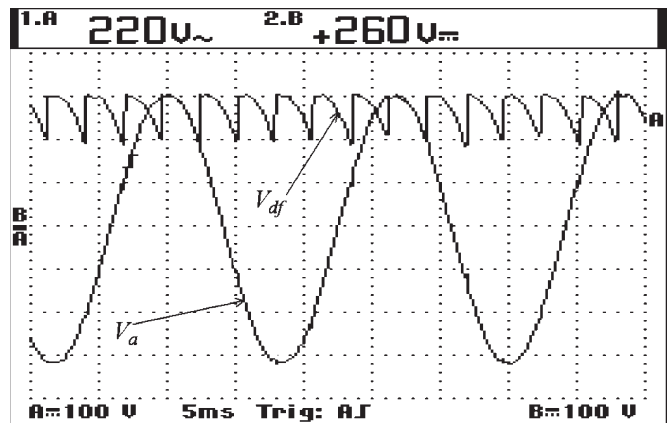


Fig. 9. Waveforms of voltage V_{df} and V_{ab} .

with respect to phase a voltage without injection of the third harmonic current. It is clear from this figure that the supply current has very high THD mostly of fifth and seventh harmonics. Fig. 11 shows the voltage of V_{dn} , and V_{fn} . It is shown in the top of the experimental result waveform that the frequency of this voltage is 180° , which is the third harmonic voltage, and the

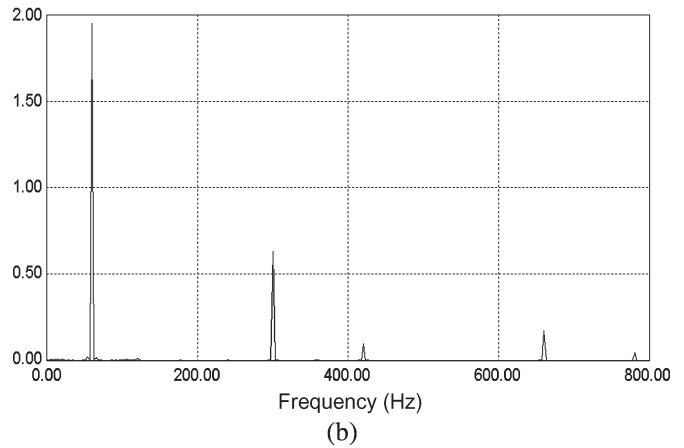
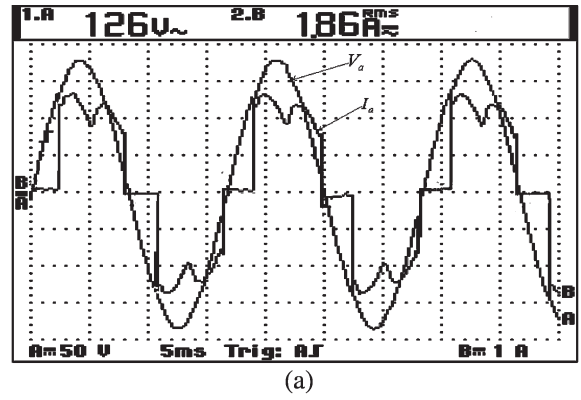


Fig. 10. Supply current waveform and its FFT components with respect to phase a voltage without injection of third harmonic current. (a) Experimental result. (b) FFT components of I_a .

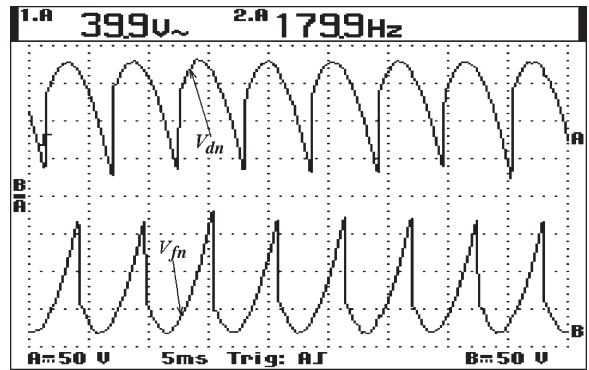
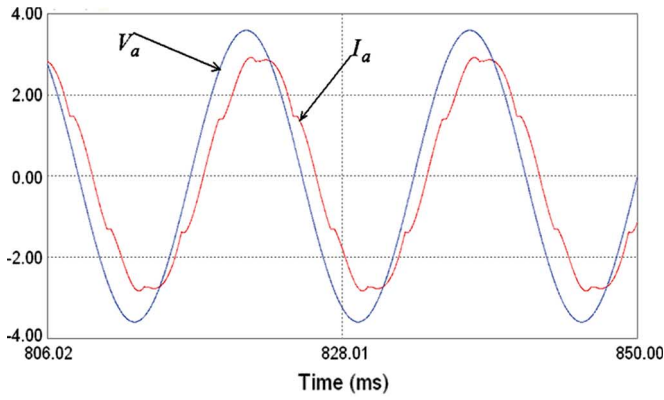


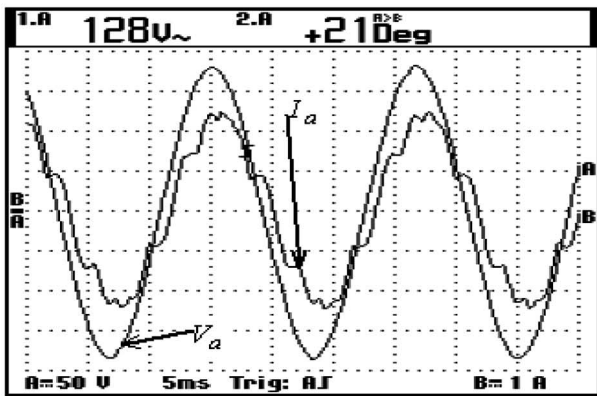
Fig. 11. Voltage of V_{dn} , and V_{fn} .

value of rms voltage is 39.9, which can be obtained from (10) at $\alpha = 20^\circ$. Fig. 12 shows the supply current waveform and its FFT components with respect to the phase a voltage with optimum amplitude and angle of the third harmonic current injection. It is clear from this figure that the supply current comes very near to the sine-wave with 5% THD.

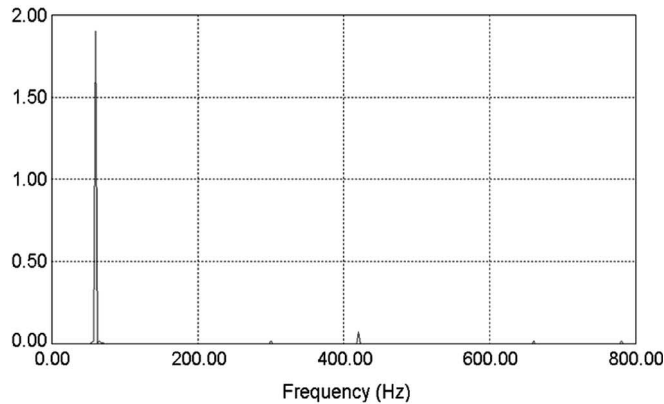
Fig. 13 shows the supply current waveform I_a and the optimum value and angle of injection of the third harmonic current with respect to the phase a voltage. It is clear from these waveforms that the value of the angle between I_f and V_a is about 120° and the angle between I_a and I_f is 180° which agree with the vector diagram shown in Fig. 4(a).



(a)



(b)



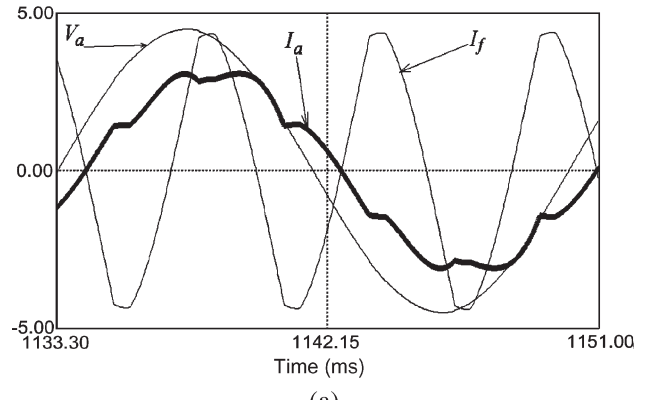
(c)

Fig. 12. Supply current waveform and its FFT components with respect to phase a voltage at optimum third harmonic current injection. (a) Simulation result. (b) Experimental result. (c) FFT components of I_a .

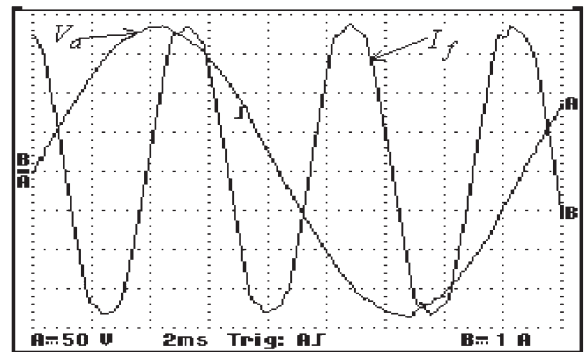
B. Simulation and Experimental Results at $\alpha = 40^\circ$

Fig. 14 shows the waveforms of voltage V_{df} and V_{ab} . Fig. 15 shows the supply current waveform and its FFT components along with phase a voltage without injection of the third harmonic current. It is clear from this figure that the supply current has very high THD mostly of fifth and seventh harmonics. It is clear that this THD is higher than the one with $\alpha = 40^\circ$.

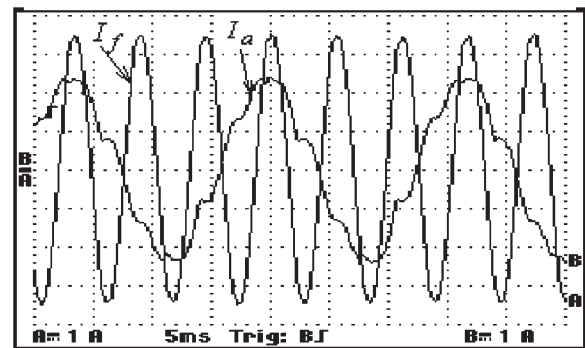
Fig. 16 shows the voltage of V_{dn} and V_{fn} and their FFT components with respect to phase a voltage. It is clear from this figure that these voltages have triplex harmonics and the third harmonic is the most dominant. It is also clear that both voltages V_{dn} , and V_{fn} have the same harmonics.



(a)



(b)



(c)

Fig. 13. Supply current waveform I_a and optimum value and angle of injection third harmonic current with respect to phase a voltage. (a) Simulation result for V_a and I_f . (b) Experimental result for V_a and I_f . (c) Experimental result for I_a and I_f .

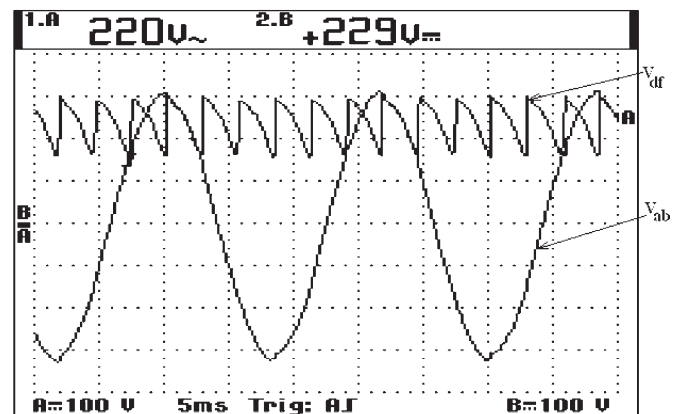
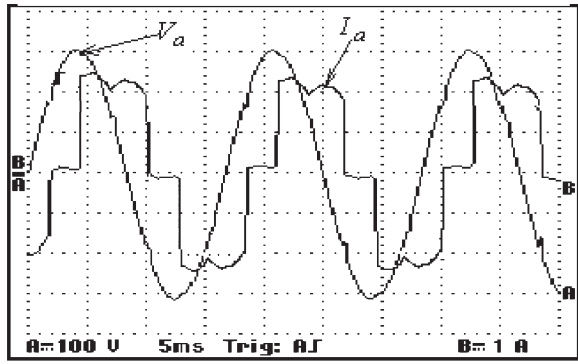
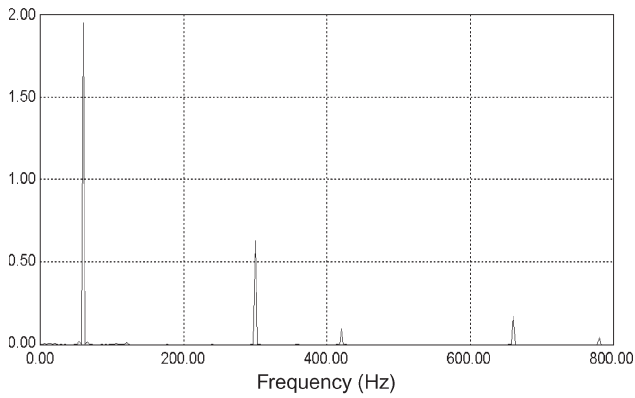


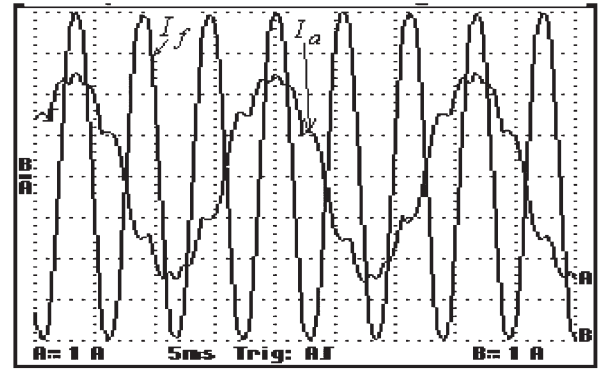
Fig. 14. Waveforms of voltage V_{df} and V_{ab} .



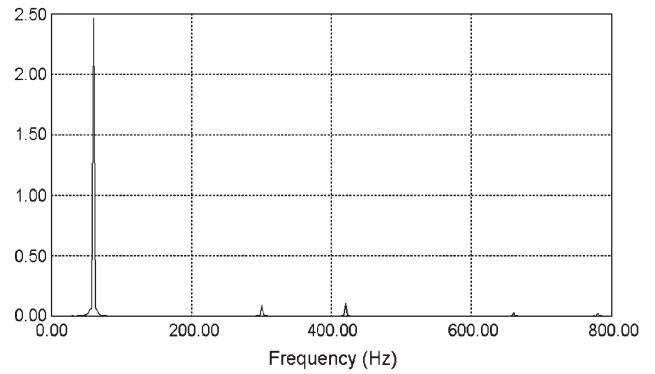
(a)



(b)



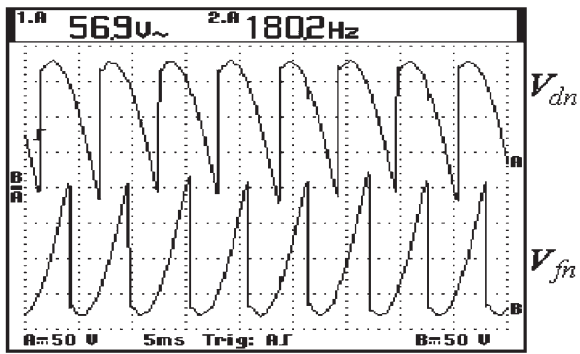
(a)



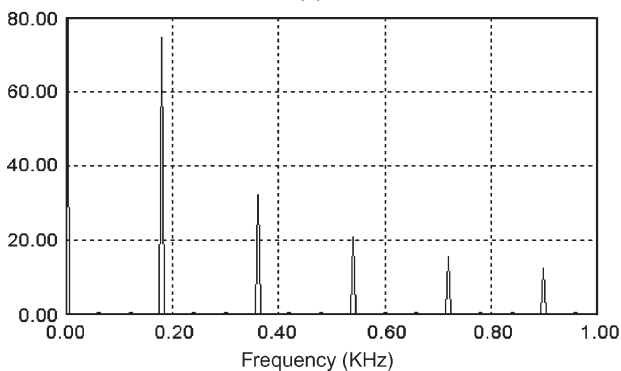
(b)

Fig. 15. Supply current waveform and its FFT components along with phase a voltage without injection of third harmonic current. (a) Experimental result. (b) FFT components of I_a .

Fig. 17. Supply current waveform and its FFT components with optimum value and angle of injection third harmonic current. (a) Experimental result. (b) FFT components of I_a .

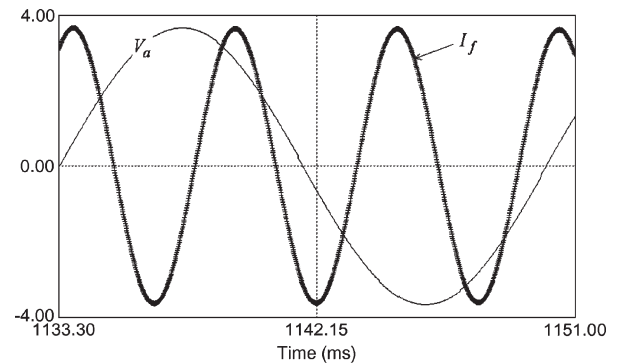


(a)

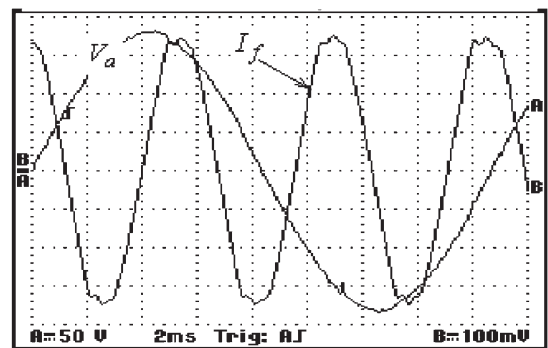


(b)

Fig. 16. Voltage of V_{dn} , and V_{fn} and their FFT components with respect to phase a voltage. (a) Experimental result. (b) FFT components of V_{dn} and V_{fn} .



(a)



(b)

Fig. 18. Supply current waveform I_a and optimum value and angle of injection third harmonic current with respect to phase a voltage. (a) Simulation result. (b) Experimental result.

Fig. 17 shows the supply current waveform and its FFT components with optimum value and angle of injection of the third harmonic current. It is clear from this figure that the supply current comes very near to the sine-wave with 6% THD.

Fig. 18 shows the supply current waveform I_a and optimum value and angle of the third harmonic injection current with respect to phase a voltage. It is clear from these waveforms that the angle between I_f and V_a is about 60° , which agree with the vector diagram in Fig. 4(b).

V. CONCLUSION

The third harmonics injection technique plays a significant role in reducing the THD of the utility line current of three-phase controlled converters. The optimal amplitude and phase angle of the injection current changes with the firing angle. In this paper, a detailed analysis for determining the relation between the optimal amplitude and phase angle of the injection current along with the firing angle has been carried out. The THD of line current is highly affected by the amplitude of the third harmonic injection current as well as its phase angle with the supply voltage. The optimum amplitude and angle of the third harmonic current have been determined by a detailed mathematical analysis of the system. The THD of the utility line current from the simulation and experimental results proves the mathematical results for this technique. The THD of the utility line current with optimal harmonic injection current is lower than the limits of harmonics standards.

REFERENCES

- [1] V. Nedici and T. A. Lipo, "Low-cost current-fed PMSM drive system with sinusoidal input currents," *IEEE Trans. Ind. Appl.*, vol. 42, no. 3, pp. 753–762, May/June 2006.
- [2] W. Farrer, "Significant source harmonic reduction achieved using direct parallel connection of two 6-pulse converters," *Proc. Inst. Electr. Eng.—Electr. Power Appl.*, vol. 153, no. 2, pp. 167–176, Mar. 2006.
- [3] K. Mukherjee, S. SenGupta, T. K. Bhattacharya, A. K. Chattopadhyay, and S. N. Bhadra, "Simplified analytical averaged model of a thyristorized commutatorless series motor," *IEEE Trans. Ind. Appl.*, vol. 42, no. 6, pp. 1508–1515, Nov./Dec. 2006.
- [4] A. I. Maswood, A. K. Yusop, and M. A. Rahman, "A novel suppressed-link rectifier-inverter topology with near unity power factor," *IEEE Trans. Power Electron.*, vol. 17, no. 5, pp. 692–700, Sep. 2002.
- [5] R. Naik, N. Mohan, M. Rogers, and A. Bulawka, "A novel grid interface, optimized for utility-scale applications of photovoltaic, wind-electric, and fuel-cell systems," *IEEE Trans. Power Del.*, vol. 10, no. 4, pp. 1920–1926, Oct. 1995.
- [6] N. Mohan, "A novel approach to minimize line current harmonics in interfacing renewable energy sources with 3-phase utility systems," in *Proc. IEEE Conf. APEC*, Boston, MA, Feb. 1992, pp. 852–858.
- [7] H. A. Pacheco, G. Jimenez, and J. Arau, "Optimization method to design filters for harmonic current reduction in a three phase rectifier," in *Proc. IEEE Conf. CIEP*, Puebla, Mexico, Aug. 1994, pp. 138–144.
- [8] S. Bhattacharya, D. M. Divan, and B. B. Banerjee, "Control and reduction of terminal voltage harmonic distortion (THD) in hybrid series active and parallel passive filter system," in *Proc. IEEE PESC*, Seattle, WA, Jun. 1993, pp. 779–786.
- [9] J. Ortega, M. Esteve, M. Payán, and A. Gómez, "Reference current computation methods for active power filters: Accuracy assessment in the frequency domain," *IEEE Trans. Power Electron.*, vol. 20, no. 2, pp. 446–456, Mar. 2005.
- [10] B. Lin and Y. Ou, "Active power filter based on three-phase two-leg switch-clamped inverter," *Electr. Power Syst. Res.*, vol. 72, no. 1, pp. 63–72, Nov. 2004.
- [11] S. Bhattacharya, P. Cheng, and D. M. Divan, "Hybrid solutions for improving passive filter performance in high power applications," *IEEE Trans. Ind. Appl.*, vol. 33, no. 3, pp. 732–747, May/June 1997.
- [12] B. S. Lee, P. N. Enjeti, and I. J. Pitel, "An optimized active interphase transformer for auto-connected 12-pulse rectifiers results in clean input power," in *Proc. IEEE Conf. APEC*, Atlanta, GA, Feb. 1997, vol. 2, pp. 666–671.
- [13] S. Choi, P. N. Enjeti, H. Lee, and I. I. Pital, "A new active interface reactor 12-pulse rectifiers provides clean power utility interface," *IEEE Trans. Ind. Appl.*, vol. 32, no. 6, pp. 1304–1311, Dec. 1996.
- [14] B. S. Lee, "New clean power reactor systems for utility interface of static converters," Ph.D. dissertation, Texas A&M Univ., College Station, TX, Aug. 1998.
- [15] C. T. Tinsley, "Modeling of multi-pulse transformer rectifier units in power distribution systems," M.S. thesis, Virginia Polytechnic Inst., Blacksburg, VA, Aug. 2003.
- [16] A. Ametani, "Harmonic reduction in thyristor converters by harmonic current injection," *IEEE Trans. Power App. Syst.*, vol. PAS-95, no. 2, pp. 441–450, Mar./Apr. 1976.
- [17] P. Pejovic, "Two three-phase high power factor rectifiers that apply the third harmonic current injection and passive resistance emulation," *IEEE Trans. Power Electron.*, vol. 15, no. 6, pp. 1228–1240, Nov. 2000.
- [18] M. Rastogi, N. Mohan, and C. P. Henze, "Three-phase sinusoidal current rectifier with zero-current switching," *IEEE Trans. Power Electron.*, vol. 10, no. 6, pp. 753–759, Nov. 1995.
- [19] P. Pejovi and D. Shmilovitz, "Low-harmonic thyristor rectifiers applying current injection," *IEEE Trans. Aerosp. Electron. Syst.*, vol. 39, no. 4, pp. 1365–1374, Oct. 2003.
- [20] S. Pal, "Simulation of current mode control schemes for power factor correction circuits," M.S. thesis, Faculty Eng. Appl. Sci., Memorial Univ. Newfoundland, St. John's, NF, Canada, May 1998.
- [21] C. Rech and J. R. Pinheiro, "Line current harmonics reduction in multi-pulse connection of asymmetrically loaded rectifiers," *IEEE Trans. Ind. Electron.*, vol. 52, no. 3, Jun. 2005.
- [22] J. Marafao, J. Pomilio, and G. Spiazzi, "Improved three-phase high-quality rectifier with line-commutated switches," *IEEE Trans. Power Electron.*, vol. 19, no. 3, pp. 640–648, May 2004.
- [23] W. Mielczarski, W. B. Lawrance, R. Nowacki, and D. G. Holmes, "Harmonic current reduction in three-phase bridge-rectifier circuits using controlled current injection," *IEEE Trans. Ind. Electron.*, vol. 44, no. 5, pp. 604–611, Oct. 1997.
- [24] P. Pejovic, P. Bozovic, and D. Shmilovitz, "Low-harmonic, three-phase rectifier that applies current injection and a passive resistance emulator," *IEEE Power Electron Lett.*, vol. 3, no. 3, pp. 96–100, Sep. 2005.
- [25] A. M. Eltamaly, "A new relation between firing angle of three-phase controlled converter and best angle of injection current," in *Proc. IEEE MEPCON*, Shebin El-Kom, Egypt: Minoufiya Univ., Dec. 2003, pp. 793–798.
- [26] N. Mohan, M. Rastogi, and R. Naik, "Analysis of a new power electronics interface with approximately sinusoidal 3-phase utility currents and a regulated dc output," *IEEE Trans. Power Del.*, vol. 8, no. 2, pp. 540–546, Apr. 1993.
- [27] J. Arrillaga, Y. H. Liu, L. B. Perera, and N. R. Watson, "A current reinjection scheme that adds self-commutation and pulse multiplication to the thyristor converter," *IEEE Trans. Power Del.*, vol. 21, no. 3, pp. 1593–1599, Jul. 2006.
- [28] H. Mao, F. C. Y. Lee, D. Boroyevich, and S. Hiti, "Review of high-performance three-phase power-factor correction circuits," *IEEE Trans. Ind. Electron.*, vol. 44, no. 4, pp. 437–446, Aug. 1997.
- [29] B. Singh, B. N. Singh, A. Chandra, K. Al-Haddad, A. Pandey, and D. P. Kothari, "A review of three-phase improved power quality ac-dc converters," *IEEE Trans. Ind. Electron.*, vol. 51, no. 3, pp. 641–660, Jun. 2004.
- [30] *PSIM6.1*. [Online]. Available: www.powersimtech.com



Ali M. Eltamaly was born in Eldakahlia, Egypt, on June 28, 1969. He received the B.S. (with distinction and honor degree), M.Sc., and Ph.D. degrees from Elminia University, Elminia, Egypt, in 1992, 1996, and 2000, respectively.

He joined the Electrical Engineering Department, Texas A&M University, College Station, as a visitor from 1997 to 2000. He was a member of the Faculty of the College of Engineering, Elminia University, from 1993 to 2005. He moved to Elmansoura University, Elmansoura, Egypt, in June 2005. He is

currently a member of the College of Engineering of King Saud University, Riyadh, Saudi Arabia, since October 2005. His research interests are in the area of power electronics, motor drives and renewable energy, where he cosupervised a number of M.Sc. and Ph.D. thesis and published about 30 papers, two books, and number of technical projects.